

# Categorical evidence, confidence, and urgency during probabilistic categorization



Kurt Braunlich\*, Carol A. Seger

*Cognitive Psychology and Molecular, Cellular and Integrative Neurosciences, Colorado State University, Fort Collins, CO, USA*

## ARTICLE INFO

### Article history:

Received 6 May 2015

Accepted 4 November 2015

Available online 10 November 2015

### Keywords:

Categorization  
Decision-making  
Attention  
Confidence  
fMRI

## ABSTRACT

We used a temporally extended categorization task to investigate the neural substrates underlying our ability to integrate information over time and across multiple stimulus features. Using model-based fMRI, we tracked the temporal evolution of two important variables as participants deliberated about impending choices: (1) categorical evidence, and (2) confidence (the total amount of evidence provided by the stimuli, irrespective of the particular category favored). Importantly, in each model, we also included a covariate that allowed us to differentiate signals related to information accumulation from other, evidence-independent functions that increased monotonically with time (such as urgency or cognitive load). We found that somatomotor regions tracked the temporal evolution of categorical evidence, while regions in both medial and lateral prefrontal cortex, inferior parietal cortex, and the striatum tracked decision confidence. As both theory and experimental work suggest that patterns of activity thought to be related to information-accumulation may reflect, in whole or in part, an interaction between sensory evidence and urgency, we additionally investigated whether urgency might modulate the slopes of the two evidence-dependent functions. We found that the slopes of both functions were likely modulated by urgency such that the difference between the high and low evidence states increased as the response deadline loomed.

© 2015 Elsevier Inc. All rights reserved.

## Introduction

Decision making can be characterized as a deliberative process that involves weighing noisy samples of evidence for competing hypotheses until committing to a particular choice. Real-world decisions require decision-makers to flexibly optimize this process based on contextual demands. For instance, decision-makers must often compromise decision accuracy in order to respond quickly, a phenomenon known as the speed–accuracy trade-off (SAT), and they must often make decisions based on uncertain evidence. For example, although the consequences of either choice might be unknown, a skier heading for a tree must commit to turn left or right within a limited period of time. To be able to make advantageous decisions in such environments, decision-makers must first track the evidence for each response (the probability that each response will lead to a desirable state). Second, in order to determine whether it might be advantageous to engage in additional deliberation, make a guess based on the current evidence, or to opt out of certain trials, decision-makers must also track their decision confidence, the probability of reaching a desirable state irrespective of a particular choice (Ding and Gold, 2010; Kepecs et al., 2008; Schwartenbeck et al., 2014; Sutton and Barto, 1998). Finally, in order

to minimize costs associated with deliberation and to maximize the probability of reaching a desirable state, they must flexibly modulate their decision strategies based on the time available to respond (Cisek et al., 2009; Hanks et al., 2011; Reddi and Carpenter, 2000).

In the present study, we used an implementation of the weather-prediction categorization task in which probabilistic evidence for specific categories could unpredictably shift within single trials. This allowed us to identify neural signals associated with information accumulation and decision confidence, and to differentiate them from evidence-independent functions, such as urgency or cognitive load. Before describing our task and predictions in detail, we briefly describe the sequential sampling class of decision-making model, which provides a useful framework for conceptualizing the temporal dynamics of decision-making processes. We then describe relevant theoretical and experimental work related to the accumulation of categorical evidence and confidence. Finally, we discuss evidence-independent functions, in particular urgency, which represents a potential mechanism underlying flexible decision thresholding, and represents an important potential confound for studies designed to investigate neural mechanisms underlying the accumulation of decision evidence.

## The sequential sampling model framework

Sequential sampling models (SSMs), such as the drift diffusion model (Palmer et al., 2005; Ratcliff, 1978; Smith and Ratcliff, 2004)

\* Corresponding author at: Department of Psychology, Colorado State University, 1876 Campus Delivery, Fort Collins, CO 80523, USA.

E-mail address: [kbraunlich@gmail.com](mailto:kbraunlich@gmail.com) (K. Braunlich).

have been particularly successful in accounting for the temporal dynamics of decision-making behavior, particularly within perceptual contexts. Within this framework, the strength of evidence modulates the speed with which a decision variable (representing accumulated evidence) diffuses towards a decision boundary. The speed with which decision-makers commit to a decision is modulated both by the strength of this evidence, and by the distance between the starting point of the accumulation process and a decision threshold. One reason the SSM framework is attractive is that it provides a compelling characterization of neural activity observed in many regions of the brain.

#### *Categorical evidence*

One particularly influential body of research examined perceptual decision making in the domain of motion direction judgments; this research has shown that neuronal activity in the lateral intraparietal sulcus (area LIP) in the non-human primate tracks evidence for specific behavioral responses and shows a stereotyped pattern at the time of behavioral response, consistent with a role in accumulating evidence until a decision threshold is crossed (for review, see Gold and Shadlen, 2007). Other studies with non-human primates have shown that LIP neural activity reflects learned categorical structure (Fitzgerald et al., 2011; Freedman and Assad, 2006; Swaminathan and Freedman, 2012), and that other regions, including the primary and premotor cortices, the frontal eye fields, the superior colliculus, and the caudate also appear to accumulate categorical evidence over time (Ding and Gold, 2010, 2012; Glimcher and Sparks, 1992; Thura and Cisek, 2014). Neuroimaging studies with human participants suggest that a variety of cortical regions including the pre- and primary motor cortices and inferior temporal lobe track categorical evidence (Dunovan et al., 2014; Gluth et al., 2012; Tremel and Wheeler, 2015; Wheeler et al., 2014).

#### *Confidence*

Within the sequential sampling framework, a normative estimate of decision confidence emerges as the unsigned difference in evidence between the winning and losing response options (Kepecs et al., 2008; Pleskac and Busemeyer, 2010; Vickers and Packer, 1982). Within a biological framework, representations of confidence may be naturally derived as the unsigned difference in activity between the winning and losing category-selective neuronal pools (Insabato et al., 2010; Philiastides et al., 2010; Rolls et al., 2010a,b). Related signals have been observed in the orbitofrontal cortex (OFC), ventromedial prefrontal cortex (VMPFC), and dorsolateral prefrontal cortex (DLPFC) (Cohen et al., 2007; De Martino et al., 2013; Heekeren et al., 2006; Padoa-Schioppa, 2011; Rolls et al., 2010a,b). Although subjective estimates of confidence are likely influenced by additional sources of information, bias, and noise (Fetsch et al., 2015), this general framework provides a principled means to track the temporal evolution of confidence prior to a behavioral response; one that we adopt in the present experiment.

#### *Urgency*

The final function we review is urgency, a monotonically increasing signal hypothesized to represent an effective mechanism to modulate decision thresholds within trials (Cisek et al., 2009; Standage et al., 2014a,b, 2011; Thura et al., 2012). Previous groups have modeled urgency in two different ways. The first is via multiplicative gain modulation of the decision input, an effect predicted by theory, and one that has been observed in the neural activity of the LIP and in the pre- and primary motor cortices in the non-human primate (Cisek et al., 2009; Ditterich, 2006a,b; Standage et al., 2011; Thura et al., 2012; Thura and Cisek, 2014). The second is via an additive effect that increases baseline activity across neuronal pools (Churchland et al., 2008; Gluth et al., 2012; Hanks et al., 2014; Kira et al., 2015; Thura and Cisek, 2014). Additive effects of urgency have been observed in the neural activity of the

FEF, LIP, and in the primary and premotor cortices of the non-human primate (Churchland et al., 2008; Hanks et al., 2014; Heitz and Schall, 2012; Kira et al., 2015; Thura and Cisek, 2014).

Cisek and colleagues (Cisek et al., 2009; Thura et al., 2012; see also Simen, 2012) have noted that these evidence-independent urgency signals could be easily mistaken for signals related to the accumulation of decision evidence. In a strong formulation of their theory, observed patterns of “accumulator” activity might not reflect the accumulation of decision-evidence at all, but rather gain modulation, via an urgency signal, of low-pass filtered estimates of sensory evidence. In part to differentiate signals related to information-accumulation and urgency, several recent studies have employed tasks where the evidence for, and against, specific categorical responses can be modulated within single trials (Gluth et al., 2012; Kira et al., 2015; Thura and Cisek, 2014; Wheeler et al., 2014; Yang and Shadlen, 2007). To date, only two studies have employed fMRI to do so (Gluth et al., 2012; Wheeler et al., 2014). We feel that this is important for two reasons: first, neuronal pools that accumulate information over time participate in larger decision-making networks (e.g., Lo and Wang, 2006), and second, different neural regions likely accumulate information for different purposes, even within a single task.

Wheeler et al. (2014) adapted a temporally extended version of the weather prediction classification task used by Yang and Shadlen (2007) to compare trials in which information accumulated at different rates. They found that motor cortices were sensitive to the rate at which effector-specific evidence was presented, and that regions neighboring the occipital/temporal lobe junction and superior middle temporal gyrus were sensitive to the strength of decision evidence but were insensitive to effector information. Gluth et al. (2012) used a model-based approach in conjunction with a temporally extended, value-based decision-making task in which participants integrated evidence from multiple “+” and “−” signs in order to make advantageous financial decisions. This allowed them to identify signals tracking the value of specific choices over time (bilateral cortical motor regions) and signals that were sensitive to the prediction of reward (ventral striatum and VMPFC).

#### *Present study*

In the present experiment, we used a temporally extended version of the weather prediction task in which the features of an abstract amoeba stimulus were added to the display one-by-one over four discrete steps (Fig. 1). Each feature was associated with a different amount of probabilistic evidence for a specific category, and participants had to integrate this information both across time and across multiple stimulus features. These characteristics capture important aspects of decisions made within high dimensional real-world environments. First, real-world decision-makers often have to flexibly assign weights to information sources according to their estimated reliability, and second, they often have to consider multiple samples of noisy information to improve the accuracy of their judgments. Importantly, our experimental design allowed us to differentiate representations of categorical evidence and confidence from signals that would be expected to increase monotonically with each trial (such as the additive urgency signal or demands associated with an increasing number of stimulus features). It also allowed us to investigate whether representations of decision evidence are multiplicatively modulated by urgency.

In line with previous research, we hypothesized that the integration of categorical evidence would recruit regions of the parietal lobe (Churchland et al., 2008; Ploran et al., 2007; Ploran et al., 2011; Shadlen and Newsome, 2001; Yang and Shadlen, 2007), as well as primary and premotor regions (Gluth et al., 2012; Pastor-Bernier and Cisek, 2011; Thura and Cisek, 2014; Wheeler et al., 2014). We predicted that frontal regions, such as the VMPFC, the OFC and DLPFC would represent effector-independent decision confidence (the unsigned difference in evidence for each of the two categories; Cohen et al., 2007; De Martino et al., 2013; Heekeren et al., 2006; Padoa-Schioppa, 2011;

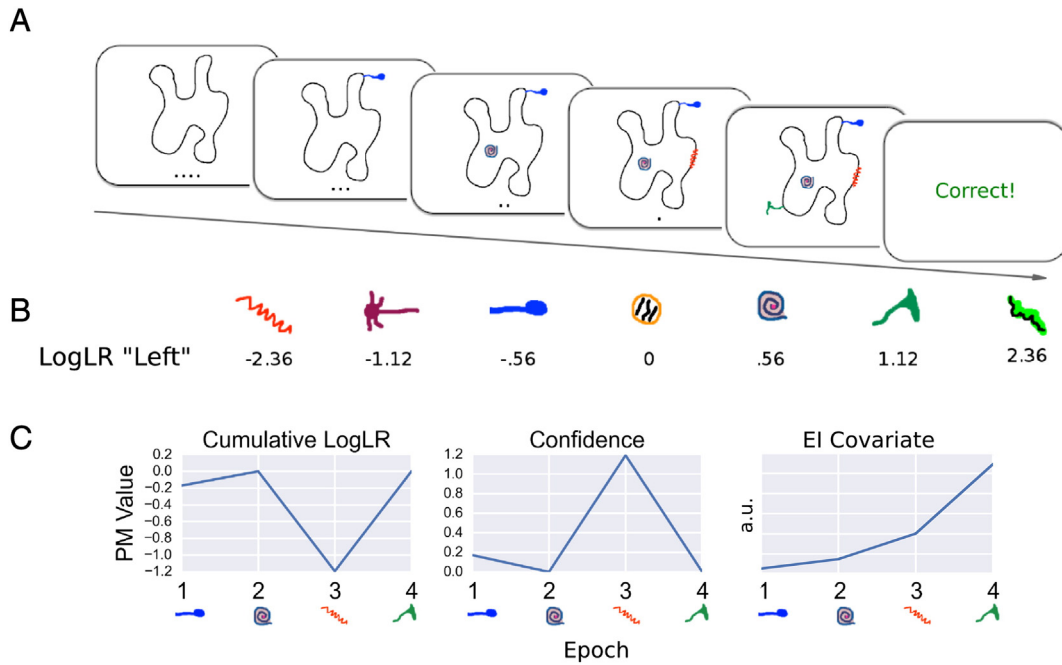


**Fig. 1.** (A) Trial format. In the scanner, each trial began with the presentation of the blank amoeba profile. The features (abstract organelles, nuclei and flagella, each representing different amounts of probabilistic evidence towards a right or left response) then accumulated over four steps. Feature onsets were separated by a jittered interval. Participants were free to respond at any time during the trial. After a response, feedback was disbursed according to Eq. (2). A series of small dots, presented below each amoeba, indicated the number of steps remaining in the trial. (B) Although the relationship between visual feature and logLR was randomized for each participant, we illustrate one possible mapping. Positive logLRs represent evidence for a response made with the left hand. (C) For this mapping between visual feature and logLR, we illustrate the cumulative logLR, confidence, and evidence-independent (EI) functions for one possible trial (individual logLRs =  $-.56, .56, -2.36, 2.36$ ). Note that although the cumulative logLR on the fourth step can be calculated via Eq. (1), due to uncertainty about impending features, an optimal representation of the evidence available on the earlier steps is less than the sum of the logLRs of the individual features (see *Definition of parametric modulators*). We tested both exponential and linear representations for the EI function; as the exponential function provided a better fit to the neuroimaging data, we used it in each model, and also illustrate it here.

Rolls et al., 2010a,b). We also predicted that urgency would multiplicatively modulate representations of categorical evidence in cortical somatomotor regions (Thura and Cisek, 2014). Finally, although we are unaware of any experimental research investigating interactions between confidence and urgency, if category-selective neuronal pools are multiplicatively modulated by urgency, and if confidence is derived from the unsigned difference in their activity (Insabato et al., 2010; Rolls et al., 2010a), it follows that representations of confidence should also show this effect.

**Methods**

*Participants*

Twenty right-handed participants (mean age = 24, SD = 4; 12 female) were recruited from the Colorado State University and University of Colorado at Boulder communities. Participants were screened for history of psychiatric and neurological disorders, for current use of psychoactive medications and for exclusionary MR criteria. All participants were compensated at a rate of \$20 per hour.

*Task*

Participants performed a temporally extended, binary, probabilistic categorization task (Wheeler et al., 2014; Yang and Shadlen, 2007) wherein they were instructed to categorize different amoeba (Fig. 1) into one of two categories: category “A” (indicated with a left hand response) and category “B” (indicated by a right hand response). For mnemonic purposes, throughout the paper, we will refer to the categories by the response with which they were associated, “left” and “right”. The amoeba stimuli consisted of a black outline upon which seven different features (such as flagella, nuclei, and organelles) could appear. Features could be repeated, and could appear at four different locations. Presenting the cues as features of an amoeba was chosen for several

reasons. First, we thought that presenting cues as features of a single object might encourage information integration and the representation of features as aspects of a single object. Second, it provided a suitable cover story, as biological kinds are often described in terms of typical features that may occur probabilistically.

At the beginning of each trial, the black outline served as an ad hoc fixation point, and cued the beginning of each trial. The features then accumulated, one-by-one, over four discrete steps. Each feature provided a different amount of probabilistic evidence towards each category. The logLRs associated with the individual features were  $-2.36, -1.12, -.56, 0, .56, 1.12,$  and  $2.36$ , where positive weights indicate evidence towards category left, and where 0 indicates no evidence towards either response. Participants were free to respond at any time during the trial, and were instructed to simply wait until they had enough information before doing so. After making a response, the features stopped accumulating, and feedback was presented. We randomized the mapping between logLR and visual feature for each participant in order to avoid possible confounds associated with visual salience. The optimal response for each trial was determined by the sign of the sum of the logLRs associated with the individual features:

$$CmLogLR_{(step4)} = \log_7 \frac{P(\text{Left} | F_1, F_2, F_3, F_4)}{P(\text{Right} | F_1, F_2, F_3, F_4)} = \sum_{i=1}^4 w_i \tag{1}$$

where  $F_{(1-4)}$  indicate the specific features of a particular amoeba and  $w_i$  the weights assigned to the individual features. Feedback was disbursed according to the corresponding probability:

$$P(\text{Left} | F_1, F_2, F_3, F_4) = \frac{7 \sum_{i=1}^4 w_i}{1 + 7 \sum_{i=1}^4 w_i} \tag{2}$$

where  $P(\text{Right}) = 1 - P(\text{Left})$ .

## Training

Participants performed two training sessions that occurred on separate days. The goals of the training sessions were to teach participants about the logLRs associated with the individual features, to teach them how to integrate information across features, and to give them experience with the temporally extended task that they would perform in the scanner. In the first training task, in order to allow participants to quickly gain experience with a large number of experimental trials, we did not use the temporally extended paradigm described above, but instead presented all features at the same time. Through trial and error, participants first learned to categorize amoeba with one, two, three, and then all four features. Feedback was disbursed according to the probability corresponding to the sum of the individual logLRs (Eq. (2)). For positive feedback, the word “correct” was presented in green for .75 s, and was accompanied by a pleasant tone. For negative feedback, the word “wrong” was shown for .75 s in red, and was accompanied by an unpleasant tone. Participants trained until they reached an 80% accuracy criterion twice (accuracy was determined in relation to an optimal classifier making decisions based on the sign of the sum of the individual logLRs; the criterion was polled every 30 correct trials, and was reset after 35). After completing this initial training task, participants then practiced the temporally extended paradigm that they would later perform in the scanner.

The second training session was completed on the same day as scanning. It was identical to the first with the exception that participants began the session by training with all four features, which were presented simultaneously. After reaching the 80% accuracy criterion (twice), they again practiced with the temporally extended paradigm.

## Scanning

In the scanner, the task was similar to the temporally extended task included during the training sessions, but both the inter-feature and inter-trial intervals were jittered. The interval between each feature (and between the last step and feedback) was jittered according to a uniform distribution with a minimum of 2 s (to mitigate nonlinear effects associated with shorter intervals; Buckner, 1998; Friston et al., 2000), and a maximum of 4 s (step size = 0.5 s; Gluth et al., 2012). The interval between each trial was jittered according to a positively skewed truncated exponential distribution ranging from 2 to 9 s.

Participants performed the task during 3 scanner runs, each of which required 14 min. As participants were free to respond at any time during the trial, the number of trials per run depended on when participants made their behavioral responses (i.e., if they tended to respond quickly, each trial tended to be shorter, and there were a greater number of trials per session). Each run involved the acquisition of 420 whole-brain volumes with an interleaved EPI 2D sequence (TR = 2,000 ms, TE = 25 ms, voxel size: 2.3 × 2.3 × 3.5, flip angle = 75°, GRAPPA acceleration factor 2). We discarded the first 2 volumes to allow for magnetization equilibration. We also collected anatomical images using an MPRAGE sequence.

## Analyses

### Preprocessing

Preprocessing involved slice-timing correction, motion correction, coregistration, high pass filtering at 128 s, segmentation of the anatomical images, and normalization of the structural and functional images to the MNI template. For the classical analyses, we smoothed the normalized images with a 6-mm full-width-at-half-maximum Gaussian kernel. For the random-effects Bayesian model selection (RFX-BMS) procedure (described below), we used the normalized unsmoothed functional images (down-sampled to 3-mm isotropic voxels to improve computational efficiency) to calculate the log-evidence maps for each model and each

participant. We smoothed the log-evidence maps with an 8-mm full-width-at-half-maximum Gaussian kernel prior to group-level analyses. All neuroimaging analyses were performed using statistical parametric mapping (SPM12; Wellcome Trust Center for Neuroimaging).

### Model-based analyses

To track the evolution of categorical evidence and confidence, and to investigate how these representations were modulated by urgency, we adopted a model-based approach. As some of these models yielded highly similar statistical maps, in order to determine which of our models best accounted for the data, we compared them using a random-effects Bayesian model selection procedure (RFX-BMS; Rosa et al., 2010; Stephan et al., 2009). This involves three steps. First, we used a classical (restricted maximum likelihood) approach to identify voxels surviving standard statistical thresholds. Second, we generated log evidence maps ( $\log P(y|m)$ , the log probability of the data,  $y$ , if it were generated by the model,  $m$ ) for each model and each participant using a variational Bayesian approach. Third, we used a random-effects analysis at the group level to calculate the protected exceedance probabilities of each model (PXP; Rigoux et al., 2014; Stephan et al., 2009). This is the probability that a given model is more frequent than any of the other models tested, above and beyond chance. Although calculation of the log evidence maps is computationally intensive, the RFX-BMS approach is attractive, as it provides an intuitive metric of model fit, allows comparison of non-nested models, and has some favorable properties when compared to the Akaike information criterion and the Bayesian information criterion (Penny, 2012; Rigoux et al., 2014).

For both the classical and Bayesian analyses, we assumed that neural activity associated with deliberation would continue across each jittered inter-feature interval, and so modeled each feature step with a duration equal to the difference between its onset and the onset of the following feature or the behavioral response. Such variable-duration epoch models tend to be more sensitive for paradigms involving cognitive events of variable duration than constant epoch or variable amplitude impulse models (Grinband et al., 2008). For all models, we used the canonical double gamma hemodynamic response function. As a default, we corrected for multiple comparisons using the topological false discovery rate (initial cluster-forming threshold:  $p < .001$ ,  $q < .05$ ; Chumbley and Friston, 2009). However, to improve our spatial estimates concerning the evidence-independent (EI) covariate (described below), we considered the more conservative familywise error rate (FWER,  $p < .05$ ).

### Definition of parametric modulators (PMs)

As feedback was disbursed based on all evidence available at the end of the trial, it was not possible to accurately calculate cumulative logLR for earlier steps by summing the logLRs for these features (as in Eq. (1)). Instead, we determined the values of steps 1–3 computationally, by tabulating the full permutation matrix (with replacement) and calculating the proportion that each partial feature sequence would be categorized as “left”. As evidence for the two categories was perfectly anticorrelated, we defined confidence as the unsigned CmLogLR (Fetsch et al., 2014; Hebart et al., 2014; Rolls et al., 2010a,b). We defined urgency as a monotonically increasing signal that peaked on the 4th step (the last step where it was possible to produce a behavioral response that would lead to positive feedback). Both linear and exponential urgency functions were tested via RFX-BMS, and because we found that the exponential function provided a better fit to the neuroimaging data, we used it for all analyses described below.

To model the multiplicative effect of urgency on categorical evidence and confidence, we multiplied them by urgency. The multiplicative effect of urgency, therefore, modulated the slope of the evidence variables such that the difference between high and low evidence states increased with each step. A limitation of our design was that we could not differentiate the additive effect of urgency from other functions that would be

expected to increase during each trial (such as increasing cognitive load associated with an increasing number of stimulus features). Accordingly, throughout the paper, we will refer to the additive urgency signal as the evidence-independent (EI) covariate to emphasize that it was included in order to control for signals that were insensitive to decision evidence. Inclusion of this covariate is important, as such monotonically increasing, but evidence-independent, signals can be easily mistaken for those associated with evidence accumulation (Simen, 2012).

To fit our models to the strategies used by individual participants, we estimated the subjective weights of evidence (sWOE) that each participant placed on the individual features (Fig. 2B). To do so in a manner robust to separation, we performed a Bayesian logistic regression analysis (prior mean = 0 for all parameters; Gelman et al., 2008). To calculate the cumulative subjective logLR, we followed a similar procedure used to calculate cumulative normative logLR; we tabulated the full permutation matrix of beta coefficients, summed each row to determine the optimal response, and then calculated the proportion that each sequence of features would be categorized as “left.” Calculation of the other subjective regressors also followed the process outlined for the construction of the normative regressors.

### Classical analyses

As mentioned, a primary focus of the present study was to differentiate signals related to information accumulation from evidence-independent functions related to urgency or cognitive load. However, we were also interested in investigating how urgency might modulate representations of decision evidence. To do so, we built four models to track the temporal evolution of CmLogLR, confidence and the EI covariate. Each model included two PMs per mean feature regressor. The first tracked decision evidence (model 1, CmLogLR; model 2, the multiplicative interaction between CmLogLR and urgency; model 3, confidence; model 4, the multiplicative interaction between confidence and urgency), while the second PM tracked the EI covariate. We were thus able to investigate multiplicative effects of urgency via the first PM, and control for the EI covariate via the second. Importantly, in order to limit our inferences to the unique variance associated with each regressor, we did not orthogonalize them (Mumford et al., 2015) so that any shared variance would be included in the error term rather than the first PM. Our design thus allowed us to differentiate signals related to the strength of decisional evidence (categorical evidence and confidence) from task-related signals that increased monotonically during each trial.

### Random-effects Bayesian model selection (RFX-BMS)

As there was considerable overlap between the statistical maps derived from some of the classical analyses, we conducted two RFX-BMS analyses. The first compared categorical evidence to categorical evidence multiplicatively modulated by urgency. The second compared confidence to confidence multiplicatively modulated by urgency. For each model, we included one PM per mean regressor. We limited these analyses to voxels within binary masks that included all significant voxels from the corresponding classical statistical maps. This approach allowed us to compare models within a single framework, to use RFX-BMS to inform our interpretations of the classical statistical maps, and to limit our inferences to voxels surpassing standard statistical thresholds. In Figs. 3C, 4C, and 5B, we thresholded each PXP map to include only voxels where the model provided the best fit. These thresholded maps allow the reader to quickly identify voxels best accounted for by each model, and to make inferences about the strength of the evidence relative to the other model tested.

## Results

### Behavioral results

Average accuracy (determined relative to an optimal classifier making decisions based on the sign of the cumulative normative logLR on

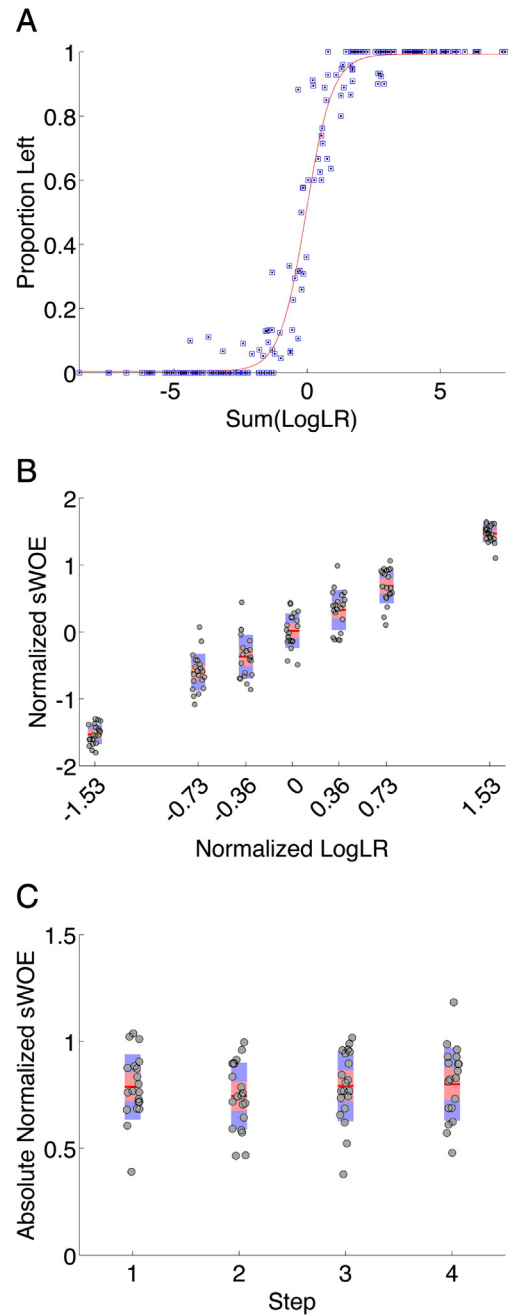


**Fig. 2.** Behavioral performance. (A) For each participant, the proportion of category left responses is plotted across 10 bins of summed cumulative normative LogLR (Eq. (1)). (B) Normalized subjective weights of evidence (sWOE) vs. the normalized normative logLR used to determine the probabilistic disbursement of feedback. X-axis, normalized logLR; Y-axis, normalized sWOE derived from each participant's pattern of behavioral performance (gray dots represent individual subject estimates; dark red = mean; light red = 95% confidence interval; blue = 1 SD). (C) Influence of each step on choice: Y-axis, absolute normalized mean sWOE for each step. These analyses provide evidence that subjects tended to integrate information across features according to a weighting scheme that closely approximated the normative logLRs.

the last step) was 85% correct (SD = 6.34%). Participants were fairly conservative, and showed a strong tendency to wait until they saw all features before making a behavioral response (average response step = 3.77, SD = 0.25). To confirm that participants used a strategy wherein they weighted the features according to their reliability rather than using a simpler strategy (e.g., counting the features belonging to each category, or considering only the most informative features; Gluck et al., 2002), we conducted a logistic regression analyses (described above). The normalized beta weights for each participant are

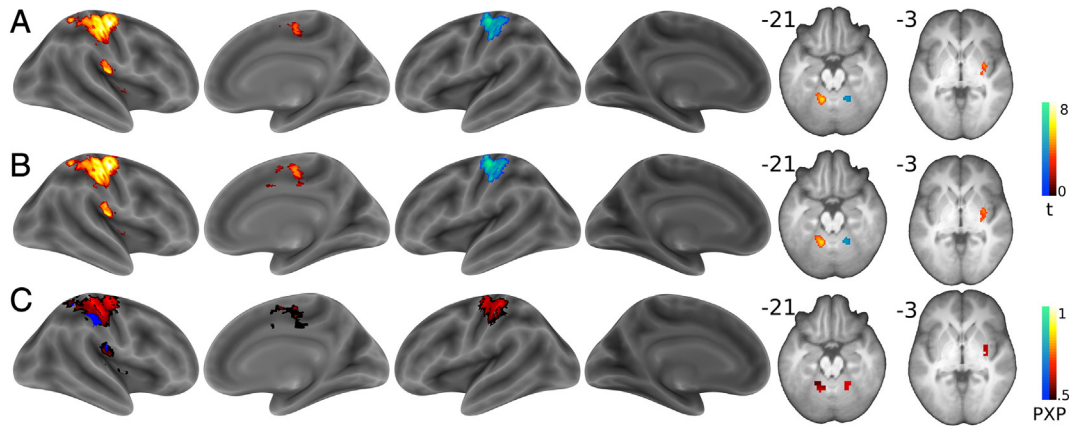


**Fig. 3.** Categorical evidence. (A) Classical results related to the categorical evidence PM. Cortical (bilateral pre- and postcentral motor regions) and cerebellar (lobules 4–5) somatomotor regions tracked the evolution of categorical evidence. Posterior regions of the right putamen, and regions of the right middle cingulate/SMA additionally tracked evidence specifically for the left category. (B) Classical results: the model tracking the multiplicative interaction between categorical evidence and urgency yielded a similar statistical map. (C) RFX-BMS results: protected exceedance probability (PXP) maps for the categorical evidence models. The PXP indicates the probability that the model is more frequent in the population (relative to the other model tested), above and beyond chance (Rigoux et al., 2014). Warm colors: CmLogLR multiplicatively modulated by urgency. Cool colors: CmLogLR. This analysis provided evidence supporting the model tracking the multiplicative interaction between categorical evidence and urgency. Slight differences in the shapes of the ROIs between the classical and RFX-BMS maps are due to differences in voxel dimensions used for these analyses.

plotted against the normalized normative logLR in Fig. 2B. The linear pattern and close correspondence between the two sets of estimates provides evidence that participants applied weights closely resembling the normative logLR used to determine the disbursement of feedback. We additionally conducted a logistic regression analysis to investigate whether participants placed greater weights on the evidence presented in particular steps (Fig. 2C), and found no evidence of such an effect,  $F(3,76) = 0.48$ ,  $p = 0.7$ ; Bayes factor in favor of the null hypothesis = 8.87. Note that this latter logistic regression analysis does not provide information about the effect of the EI covariate on the cumulative logLR (the optimal representation of current evidence), but rather provides information about the weights that participants placed on the individual features in each epoch.

#### Neuroimaging results

To reduce the number of models compared, we first investigated whether the normative or subjective CmLogLR provided a better fit to the neuroimaging data using RFX-BMS. Although the normative and subjective models were highly correlated and yielded similar maps, we found stronger evidence for the normative model, and report results related to these weights for all remaining neuroimaging analyses. We

then compared linear and exponential functions for the EI covariate. We found stronger evidence for the exponential function, and so included this function in all models described below. Finally, we tested whether the additive effect of urgency (the EI covariate) and the multiplicative effect of urgency on the normative representations of categorical evidence and confidence were best accounted for by linear or exponential urgency functions. Here too, we found that the exponential function provided a better fit than the linear function, and report these results below.

#### Categorical evidence (CmLogLR) and its interaction with urgency

During deliberation, we found that the evidence for a left response was represented in a large contralateral region of the right pre- and postcentral gyri (overlapping BA4 and BA6) extending into the right superior parietal lobe, and in the subcortical activity of left cerebellar lobules IV and V, as well as in the right posterior putamen (Fig. 3A; Table A.1). Conversely, evidence for a right response was associated with similar patterns of spatial activity in the opposite cortical and cerebellar hemispheres. The model tracking the multiplicative interaction between categorical evidence and urgency yielded highly similar statistical maps (Fig. 3B; Table A.1). To determine which model provided a better account for the data, we compared them using RFX-BMS. As

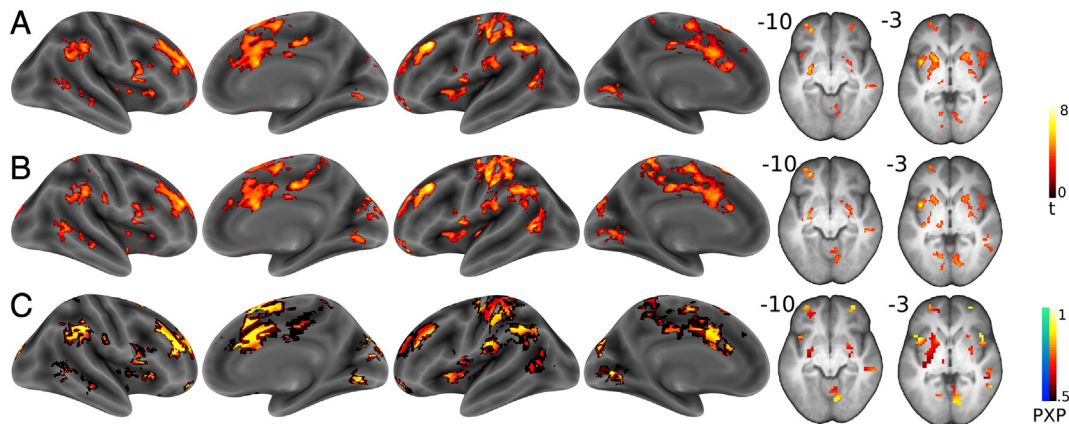


**Fig. 4.** Confidence. (A) Classical results related to the confidence PM. (B) Classical results related to the multiplicative interaction between confidence and urgency. (C) Protected exceedance probability (PXP) maps for the confidence models (CmLogLR vs. CmLogLR multiplicatively modulated by urgency). Warm colors: confidence modulated by urgency. No voxels were best fit by the confidence function that was not modulated by urgency. These results indicate strong evidence that urgency modulated the slope of the confidence signal. Slight differences in the shapes of the ROIs between the classical and RFX-BMS maps are due to differences in voxel dimensions used for these analyses.

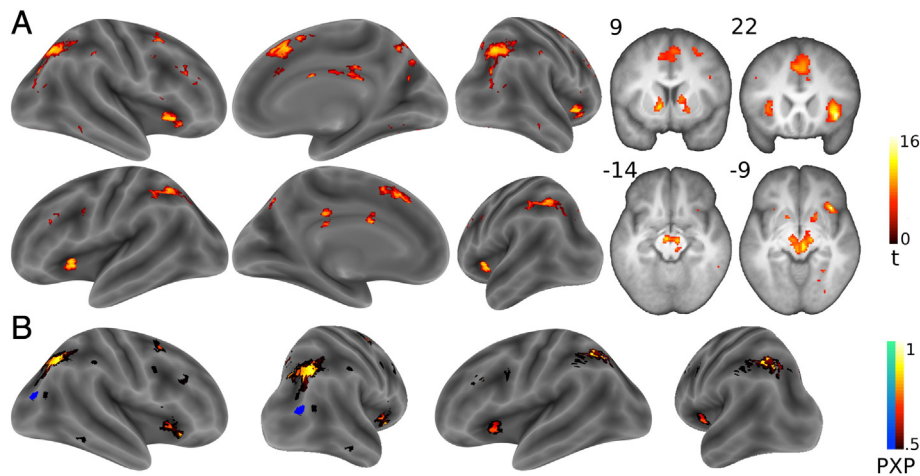


**Fig. 5.** (A) The evidence-independent (EI) covariate. We modeled the EI covariate as an exponentially increasing signal that peaked on the last step. It was included as the second PM in each model, and thus modeled shifts in baseline activity without regard to decisional evidence. Voxels were selected based on a conjunction analysis across each of the four models, and the values reflect averaged  $t$  values across these maps. To increase the precision of these spatial estimates, we corrected for multiple comparisons using the voxelwise FWER ( $p < .05$ ; note also the increased range of the color scale). Activity in the bilateral SMA and anterior insular cortices, as well as ventral striatum, midbrain, and bilateral intraparietal sulcus positively covaried with the EI covariate. (B) RFX-BMS analysis designed to investigate the effect of confidence in the IPS (for consistency with Figs. 3C and 4C, we illustrate all voxels included in 5A). Warm colors illustrate a model with 1 PM: the EI covariate. Cool colors illustrate a model including 2 PMs: (1) confidence multiplicatively modulated by urgency, and (2) the EI covariate. These results suggest that the univariate BOLD response in the bilateral regions of the IPS did not covary with the strength of decision evidence but instead tracked the EI covariate. As noted above, slight differences in the shapes of the ROIs between the classical and RFX-BMS maps are due to differences in voxel dimensions used for these analyses.

shown in Fig. 3C, we found that almost all voxels associated with the two maps were best fit by the function which was multiplicatively modulated by urgency (peak PXP  $> .75$ ). If we were to assume that one of the two functions is more frequent in the population (a common assumption for model comparison analyses), our results strongly suggest that it would be the multiplicative interaction between categorical evidence and urgency (peak unprotected exceedance probability  $> .98$ ; compare to Daw et al., 2011; den Ouden et al., 2010). To confirm that these results were not related to the behavioral response, we repeated this analysis but considered only the parametric effects for the non-response steps (the steps during which participants made a behavioral response were included in the model, but as a covariate of no interest without parametric modulation); we again found that the model tracking the multiplicative interaction between categorical evidence and urgency was more likely.

#### Confidence and its interaction with urgency

We found that confidence was represented in the activity of two large clusters in the bilateral middle frontal gyri, bilateral anterior insular cortices, bilateral SMA extending to the middle-cingulate, bilateral OFC, bilateral inferior parietal cortices, bilateral putamen and cerebellar lobules 4–6 (Fig. 4A; Table A.2). The multiplicative interaction between confidence and urgency was associated with a highly similar statistical map (Fig. 4B; Table A.2). RFX-BMS analyses indicated evidence favoring the multiplicative model across all voxels. This effect was particularly strong in regions including the bilateral SMA and inferior parietal lobes, the right middle frontal gyrus, and the right insula (peak PXP  $> .99$ ; Fig. 4C; Table A.3).

#### The evidence-independent (EI) covariate

As described above, for each of the four classical models, we included 2 PMs per mean regressor. The first PM tracked an evidence variable (categorical evidence, confidence, or the multiplicative interaction of each with urgency), and the second PM tracked evidence-independent signals that increased exponentially within each trial (Fig. 1C). A limitation of our design was that signals related to this second PM could not be ascribed to a single functional role (i.e., the additive effect of urgency could not be differentiated from other exponentially increasing signals). Importantly, however, this design allowed us to differentiate signals

that were sensitive to the strength of the decision evidence from those that were not. It also allowed us to identify activity within regions that tracked the strength of decision evidence, but also tended to increase with time (i.e., voxels that were significantly associated with both the first and second PM). Similar multiplexed signals have been previously observed in the LIP, and in the primary and premotor cortices of the non-human primate (Churchland et al., 2008; Thura and Cisek, 2014). We describe results related to the EI covariate for two reasons. First, our results indicate that signals tracking the EI covariate could be easily mistaken for those tracking uncertainty or confidence. Second, we believe that an important goal for future research will be to characterize the functional roles of this task-related variance.

As we found strong, widespread activation associated with this regressor, we corrected for multiple comparisons using the more conservative FWER ( $p < .05$ ). The resulting statistical map (Fig. 5; Table A.5) showed particularly strong peaks in the bilateral anterior insula, SMA, bilateral ventral striatum, bilateral substantia nigra, superior colliculus, regions of the cerebellum (crus II and lobule 6), and bilateral intraparietal sulcus. The map showed a fairly high degree of overlap with the confidence signal in regions of the salience network (compare with Fig. 4), particularly in the pre-SMA and bilateral insula; activity within these regions was sensitive to strength of the decision evidence and also tended to increase with each step. The model comparison analysis indicated that, for all of these voxels, the slope associated with these representations of confidence was modulated by urgency, such that the difference between the high and low evidence states increased exponentially during each trial (see Fig. 4C).

Notably, this analysis suggested that the bilateral IPS, regions that we predicted would be sensitive to decision evidence (Churchland et al., 2008; Ploran et al., 2007, 2011; Shadlen and Newsome, 2001; Yang and Shadlen, 2007), tracked the EI function instead. We found that this signal could be easily mistaken for confidence as, when we orthogonalized the EI covariate with respect to confidence (thus assigning shared variance to the confidence PM; see Mumford et al., 2015), the IPS appeared to track both confidence and urgency. To investigate whether the BOLD response in the IPS was sensitive to the strength of decision evidence, we conducted an RFX-BMS analysis in which we compared a full model, which included a PM tracking confidence and a PM tracking the EI function, to a reduced model, which tracked only the EI

covariate. Results from this analysis provided evidence confirming that activity in the bilateral IPS was best accounted for by the EI function alone (bilateral peak PXPp > .90; Fig. 5B).

## Discussion

We used a temporally extended design to investigate how participants integrated probabilistic featural information across time in order to make advantageous decisions. Importantly, although most of the features were informative, they were not perfectly predictive. This kind of probabilistic decision-making task is common in everyday life; environmental cues often provide only incomplete information about the course of action that will lead to a desired state. In order to make advantageous decisions within such environments, decision-makers must assign weights to information sources according to a weighting scheme that approximates the relevant characteristics of the external environment (Nosofsky et al., 2012; Nosofsky, 1986; Sigala and Logothetis, 2002). In the present experiment, our goal was to investigate the neural mechanisms underlying our capacity to integrate information across stimulus features of varying reliability, and to investigate how we modulate this process based upon the time available to respond. Specifically, our design allowed us to differentiate signals related to the temporal evolution of categorical evidence and decision confidence from other functions that increase monotonically during each trial without regards to the strength of the decision evidence. Finally, we were also able to investigate whether urgency modulated the slopes of the two evidence-dependent functions (categorical evidence and confidence).

### *Multi-cue integration and categorization*

A primary goal of our study was to examine how fundamental decision-making mechanisms were adapted for categorical decision making. We utilized a multiple cue probabilistic classification task in which participants integrated information across individual features according to a weighting scheme that closely approximated the normative weights used to disburse feedback (Fig. 2). Previous work provides evidence that participants sometimes use heuristic strategies based on the consideration of only the most informative features when performing the weather prediction task (Gluck et al., 2002; Meeter et al., 2006). The extensive training in our task, and the temporally extended paradigm wherein participants were exposed not only to the uncertainty associated with the informational content of the features but also to the uncertainty about what features would compose the final stimulus, may have encouraged participants to consider each of the individual features during deliberation.

### *Categorical evidence*

We found that evidence supporting a specific category and its associated response was tracked by somatomotor regions including primary motor cortex, primary somatosensory cortex, posterior putamen, and cerebellum. Activity appeared to be effector specific, such that activity within cortical somatomotor regions was positively correlated with evidence towards the contralateral response, while activity within somatomotor regions of the cerebellum was positively correlated with evidence for the ipsilateral response, consistent with the crossed nature of cortical-cerebellar projections. These observations fit with an intentional framework where these decisions can be made with regards to propositions concerning potential behavioral responses (Gold and Shadlen, 2003; Shadlen et al., 2008). Additionally, procedural category learning mechanisms are often effector specific (Cantwell et al., 2015; Spiering and Ashby, 2008), and similar effector-specificity was observed in the temporally extended fMRI studies previously discussed (Gluth et al., 2012; Wheeler et al., 2014).

### *Confidence*

We modeled confidence as the unsigned difference in evidence for each category (Ding and Gold, 2010; Hebart et al., 2014; Kepecs and Mainen, 2012; Vickers and Packer, 1982) and tracked its evolution prior to decision commitment (Gherman and Philiastides, 2014). Our confidence regressor, therefore, tracked the total amount of information accumulated from the amoeba stimulus, without regards to specific motor responses. Such a signal may play several important roles. On difficult trials, it may allow decision-makers to opt out and choose safe bets, rather than gambling on risky choices (Gherman and Philiastides, 2014; Kepecs et al., 2008; Kiani and Shadlen, 2009). It may also allow decision-makers to wait for an appropriate amount of time for probabilistic reward (Kepecs and Mainen, 2012; Kepecs et al., 2008; Lak et al., 2014). Additionally, in conjunction with urgency, it may provide important information regarding the value of accumulating additional decision evidence.

Within prefrontal cortex, dorsolateral, rostromedial, ventromedial, and orbitofrontal cortical regions have been reported to be sensitive to confidence (Bowman et al., 2012; De Martino et al., 2013; Heekeren et al., 2004, 2006; Philiastides et al., 2011; Rolls et al., 2010a; Tobler et al., 2007). These regions were also active in our study, with the notable absence of the ventromedial prefrontal cortex; due perhaps to the minimal reward and value-processing demands associated with our task (Basten et al., 2010; Smith et al., 2010). Within subcortical structures, we also found that the dorsal striatum and dopaminergic mid-brain also tracked confidence. These regions are also known to be sensitive to confidence (Ding and Gold, 2010; Schwartenbeck et al., 2014), to be recruited during performance of the weather prediction categorization task specifically (Poldrack et al., 1999; Shohamy et al., 2008), and to be sensitive to categorization demands more broadly (Braunlich et al., 2015; Lopez-Paniagua and Seger, 2011; Seger et al., 2015, 2010; Waldschmidt and Ashby, 2011).

Many studies have also found decisional confidence to be associated with activity in the inferior parietal lobe and in medial frontal regions, which are commonly associated with the ventral attention or salience networks. We found that these regions, as well as the bilateral anterior insular cortices, also tracked decision confidence. Together, these regions are thought to play an important role in the bottom-up orienting of attention to salient external events (Buckner et al., 2013; Ciaramelli et al., 2008; Medford and Critchley, 2010; Menon and Uddin, 2010; Menon, 2011; Sridharan et al., 2008). It is therefore interesting to note that these regions tracked the strength of the decisional evidence provided by the stimulus, as the salience network may play an important role in assigning attentional weights to behaviorally relevant sources of information. It is also interesting to note that these regions of the medial frontal cortex and bilateral anterior insula strongly overlapped with the statistical maps representing the EI covariate, indicating that activity within these regions tracked confidence and also increased exponentially during each trial.

### *Gain modulation of the evidence-dependent functions by urgency*

There are a number of ways that flexible adjustments to the SAT may be implemented in the brain (for full review, see Bogacz et al., 2010). One mechanism is analogous to manipulation of the decision boundary itself; through modulation of the cortico-basal ganglia circuit (the “striatal” hypothesis of the SAT). Another hypothetical mechanism underlying flexible modulation of the SAT is through modulation of baseline activity of neuronal pools involved in evidence accumulation (the “changing baseline” hypothesis). At the algorithmic level (in the sense of Marr, 1982), this has the effect of moving representations of decision evidence closer to the decision threshold. The mechanism we consider in the present paper, however, is gain modulation of decision evidence, which has the effect of modulating the slopes of the evidence functions so that the differences between high and low evidence states increases

as a response deadline approaches. Mathematical models provide evidence that such a mechanism represents an effective way to modulate the temporal dynamics of deliberative processes (Cisek et al., 2009; Ditterich, 2006a; Niyogi and Wong-Lin, 2013; Standage et al., 2011, 2013; Thura et al., 2012), and experimental work has shown that activity in the LIP and in the pre- and primary motor cortices in the non-human primate closely resembles predictions made by these models (Ditterich, 2006a; Thura and Cisek, 2014).

Thus, we predicted that urgency would modulate the slope of the categorical evidence signal. We also predicted that the confidence signal would show this effect if categorical evidence is multiplicatively modulated by urgency and if confidence is at least partially derived from the unsigned difference in activity between category-selective neuronal pools. This framework is supported by theoretical and experimental work (e.g., Insubato et al., 2010; Rolls et al., 2010a), and by recent work demonstrating that modulation of response-specific representations in the premotor cortex can influence subjective estimates of confidence (Fleming et al., 2015). Our results are in accordance with this framework, as we found that representations of both categorical evidence and confidence were best fit by the functions tracking the multiplicative effects of urgency; however, more research is needed to understand the nature and loci of this modulatory signal.

Specifically, while our task imposed a strict response deadline on the fourth step, in real-world environments, decisions about *when* to decide are often more difficult. Thus, while real-world decisions often require participants to consider fine-grained differences in costs associated with deliberation and possible benefits associated with gambling on uncertain choices, our task minimized these effects and thus inflated the salience of the last step. This allowed us to model urgency as a monotonically increasing function that peaked at this step, but it should be noted that urgency functions associated with real-world decisions are likely to be more variable. In addition, as the amount of information presented during each trial was limited to four features, accurate information accumulation required participants to temper the probabilistic information provided by each partial feature sequence (i.e., the partial sets of features shown on steps 1, 2, or 3) by the uncertainty concerning the feature(s) not yet presented during each trial. Although we modeled this effect (see Fig. 1C), it is unknown whether this aspect of the task may also have interacted with representations of the urgency function.

#### *The evidence-independent (EI) covariate*

Interpretation of the EI covariate in isolation is difficult, as signals showing monotonically ramping activity might be related to multiple functions expected to increase during each trial (e.g., urgency or cognitive demands associated with an increasing number of features). The primary reason for including it in each model was to differentiate signals sensitive to the strength of the decision evidence from others that were evidence-independent. This is important, as signals reflecting information accumulation can be easily mistaken for those associated with decision thresholding (Cisek et al., 2009; Simen, 2012; Thura et al., 2012).

Our results suggest that the pattern of BOLD response we observed in the bilateral posteromedial portion of IPS may represent such a signal; we found that this region was insensitive to the strength of decision evidence, but positively covaried with the EI covariate. However, both previous fMRI studies that manipulated evidence for, and against, specific categories within single trials (Gluth et al., 2012; Wheeler et al., 2014) also did not identify patterns of activity in the IPS that would be consistent with an information-accumulation account. Wheeler et al. suggested that activity within these regions was most consistent with an account related to cognitive effort or to time on task, while Gluth et al. noted that bilateral IPS activity at the beginning of each trial inversely correlated with decision time. Taken together, these results suggest that the univariate BOLD response in the IPS may largely reflect processes associated with decision thresholding, rather than the

accumulation of decision evidence. Regardless of the function of this signal, however, these results suggest that monotonically increasing BOLD signals previously observed in the IPS during temporally extended decision-making tasks (e.g., Ploran et al., 2007, 2011) may be insensitive to the strength of decision evidence. Our results confirm, however, that other regions indicated in these studies, notably the right middle and inferior frontal gyri, the left cerebellar crus I, the bilateral anterior insula, the medial prefrontal cortex/pre-SMA, the inferior parietal lobe, and the caudate are sensitive to the strength of decision evidence.

It is important to note, however, that recent studies employing multivariate pattern analyses (MVPA) have reported success in decoding categorical representations from these regions (e.g., Christophel et al., 2012; Jeung, 2014), and individual neurons in the non-human primate homologue of the IPS (the LIP; Sereno et al., 2001), are known to track both categorical evidence and urgency (Kira et al., 2015; Yang and Shadlen, 2007). It is thus likely that these regions are sensitive to decision evidence, but that our results reflect differences between neuroimaging methods and analyses. Specifically, we suggest that the univariate BOLD response may not reflect the information accumulation processes which likely occur within these regions, but instead may reflect neuromodulatory inputs, such as urgency, that might operate broadly across neuronal populations with different stimulus tunings (Chance et al., 2002; Douglas et al., 1995; Niyogi and Wong-Lin, 2013; Salinas and Abbott, 1996; Salinas and Thier, 2000; Standage et al., 2013) and are thought to represent an important driver of the cortical hemodynamic response (Logothetis, 2008).

#### *Conclusions*

Real-world environments often require decision-makers to integrate information across time and across multiple information sources. To do so effectively, they must weigh different information channels according to their estimated reliability. They must also adjust the timing of their behavioral responses to maximize transient opportunities to reach desirable states. In the present study, we build on the small number of experiments that have used temporally extended paradigms in conjunction with fMRI to track the accumulation of decision evidence during deliberation. Through use of model-based analyses, we were able to disentangle the temporal evolution of multiple task-related signals as participants deliberated about impending choices. We found that urgency likely modulated representations of categorical evidence and confidence such that the difference between high and low evidence states tended to negatively covary with the time available to respond. We also found that the univariate signal observed in the bilateral IPS increased exponentially during each trial, but was insensitive to the strength of decision evidence, and may thus reflect a neuromodulatory effect rather than information accumulation (see also Gluth et al., 2012 and Wheeler et al., 2014). An important goal for future research will be to investigate the functional role(s) of the signal tracking the evidence-independent covariate.

#### **Conflict of interest**

The authors declare no competing financial interests.

#### **Acknowledgements**

This research was supported in part by NIH Grant R01 MH079182 to CAS, and utilized the Janus supercomputer, which is supported by the National Science Foundation (award number CNS-0821794) and the University of Colorado Boulder. We would like to thank Brian Spiering, Alex Gonzalez, Gaojie Fan, Yinghua Liu, and Andrew Dimond for their contributions to the project.

**Appendix A**

(See Table A.5.)

**Table A.1**

Classical results: categorical evidence and categorical evidence modulated by urgency. Correction for multiple comparisons was performed through consideration of the topological false discovery rate (initial cluster forming threshold:  $p < .001$ ,  $q < .05$ ).

Model	Size (mm <sup>3</sup> )	x	y	z	t	BA	Region
<b>CmLogLR (left)</b>							
2434	38	-18	54	10.6	4		Precentral_R
219	44	-20	22	6.92	48		Rolandic_Oper_R
176	6	-18	44	5.99	23		Cingulum_Mid_R
172	-14	-52	-18	5.7	19		Cerebelum_4_5_L
74	32	-2	-4	4.64	48		Putamen_R
<b>CmLogLR (right)</b>							
1151	-34	-24	58	8.95	4		Precentral_L
82	18	-50	-20	5.01	37		Cerebelum_4_5_R
<b>CmLogLR (left) * Urgency</b>							
2780	38	-18	54	11.03	4		Precentral_R
248	44	-20	20	6.91	48		Rolandic_Oper_R
261	6	-20	44	6.02	23		Cingulum_Mid_R
224	-14	-52	-20	5.58	19		Cerebelum_4_5_L
98	32	-4	-2	4.52	48		Putamen_R
<b>CmLogLR (right) * Urgency</b>							
1208	-34	-24	58	8.93	4		Precentral_L
109	18	-50	-20	5.24	37		Cerebelum_4_5_R

**Table A.2**

RFX-BMS results: CmLogLR and CmLogLR modulated by urgency. Each map was thresholded to included voxels where the model provided the best fit. The protected exceedance probability (PXP) provides an estimate of the probability that the model is more frequent in the population, above and beyond chance.

Model	Size (mm <sup>3</sup> )	x	y	z	PXP	BA	Region
<b>CmLogLR</b>							
30	48	-25	44	0.558	3		Postcentral_R
12	42	-22	14	0.522	48		Heschl_R
<b>CmLogLR * Urgency</b>							
784	36	-25	68	0.755	6		Precentral_R
352	-39	-25	65	0.731	4		Precentral_L
68	6	-22	47	0.636	23		Cingulum_Mid_R
35	21	-52	-19	0.634	37		Cerebelum_4_5_R
64	45	-25	26	0.624	48		SupraMarginal_R
64	-15	-58	-22	0.62	37		Cerebelum_6_L
31	36	-4	2	0.618	48		Putamen_R

**Table A.3**

Classical results: confidence and confidence modulated by urgency. Correction for multiple comparisons was performed through consideration of the topological false discovery rate (initial cluster forming threshold:  $p < .001$ ,  $q < .05$ ).

Model	Size (mm <sup>3</sup> )	x	y	z	t	BA	Region
<b>Confidence</b>							
1016	-32	26	40	8.01	9		Frontal_Mid_L
7901	28	-6	4	7.32	48		Putamen_R
	14	12	60	6.77	6		Supp_Motor_Area_R
	-40	8	-4	6.6	48		Insula_L
	12	-28	40	6.08	-		Cingulum_Mid_R
	-16	-26	10	5.86	-		Thalamus_L
1106	66	-48	14	7.19	22		Temporal_Mid_R
	54	-34	40	5.9	40		SupraMarginal_R
129	-12	22	60	7.17	8		Supp_Motor_Area_L
173	-28	46	-8	7.11	11		Frontal_Mid_Orb_L
1930	-50	-20	50	6.5	4		Postcentral_L
	-18	-36	64	5.37	4		Postcentral_L
173	-50	-60	8	5.96	37		Temporal_Mid_L

**Table A.3 (continued)**

Model	Size (mm <sup>3</sup> )	x	y	z	t	BA	Region
	333	-62	-24	26	5.64	48	SupraMarginal_L
	747	-18	-72	-30	5.56	-	Cerebelum_Crus1_L
		-32	-42	-32	5.29	37	Cerebelum_6_L
	109	30	54	-14	5.4	11	Frontal_Mid_Orb_R
	163	6	-54	-18	5.16	18	Vermis_4_5
	300	-14	-78	2	5.13	18	Lingual_L
	98	12	-84	24	5.09	19	Cuneus_R
<b>Confidence by Urgency</b>							
	1052	-32	26	40	7.73	9	Frontal_Mid_L
	181	-28	46	-8	7.6	11	Frontal_Mid_Orb_L
	11730	-48	-60	6	7.29	37	Temporal_Mid_L
		-12	-44	68	7.01	5	Precuneus_L
		28	-6	4	6.95	48	Putamen_R
		-40	-20	46	6.89	4	Postcentral_L
		14	-28	42	6.61	-	Cingulum_Mid_R
		-30	-8	-16	6.44	20	Hippocampus_L
		14	14	60	6.25	8	Supp_Motor_Area_R
		-52	-52	46	5.89	40	Parietal_Inf_L
		20	20	-14	5.25	11	Frontal_Sup_Orb_R
	139	-10	22	60	6.49	8	Supp_Motor_Area_L
	1332	66	-18	32	6.33	2	SupraMarginal_R
		66	-48	14	6.27	22	Temporal_Mid_R
	682	16	-84	32	6.15	19	Cuneus_R
	1724	-22	-84	-38	6.14	-	Cerebelum_Crus2_L
		-8	-46	-18	5.79	19	Cerebelum_4_5_L
		6	-70	-38	5.25	-	Vermis_8
		-36	-50	-42	4.96	-	Cerebelum_7b_L

**Table A.4**

RFX-BMS results: confidence modulated by urgency. This model was compared to the confidence model that was not modulated by urgency. Each map was thresholded to included voxels where the model provided the best fit, and no voxels were best accounted for by the unmodulated model. The protected exceedance probability (PXP) provides an estimate of the probability that the model is more frequent in the population, above and beyond chance.

Model	Size (mm <sup>3</sup> )	x	y	z	PXP	BA	Region
<b>Confidence by Urgency</b>							
	2166	3	20	44	>0.999	32	Supp_Motor_Area_L
		-33	-64	53	0.999	7	Parietal_Sup_L
		3	-7	68	0.969	6	Supp_Motor_Area_R
		-60	-22	23	0.957	48	Postcentral_L
		-27	-10	65	0.937	6	Precentral_L
		-6	-52	59	0.936	5	Precuneus_L
		-3	-28	35	0.934	23	Cingulum_Mid_L
		-48	-67	17	0.897	39	Temporal_Mid_L
	448	45	-46	56	0.999	40	Parietal_Sup_R
		57	-52	-4	0.928	21	Temporal_Inf_R
		60	-16	38	0.87	43	Postcentral_R
	879	39	35	29	0.998	46	Frontal_Mid_R
		42	20	-4	0.997	47	Insula_R
	319	-42	29	35	0.996	45	Frontal_Mid_L
		-30	53	17	0.914	46	Frontal_Mid_L
		6	-79	11	0.995	17	Calcarine_R
	69	-3	-82	17	0.987	18	Cuneus_L
	28	30	56	-4	0.986	11	Frontal_Sup_Orb_R
	568	-9	-73	5	0.98	17	Lingual_L
		-30	-67	-28	0.978	19	Cerebelum_Crus1_L
	468	-33	17	8	0.963	48	Insula_L
		-33	-13	-22	0.7	20	Hippocampus_L
	48	-3	23	59	0.952	8	Supp_Motor_Area_L
	34	9	-16	8	0.947	-	Thalamus_R
	45	-30	59	-1	0.912	11	Frontal_Sup_Orb_L
	83	-12	-19	8	0.902	-	Thalamus_L
	19	-51	-73	11	0.876	37	Occipital_Mid_L
	39	57	-31	-7	0.867	21	Temporal_Mid_R
	33	9	-49	59	0.832	5	Precuneus_R

**Table A.5**

Classical results: the evidence-independent (EI) function. Voxels included in this map represent a conjunction analysis across the four classical models tested. *T* values reflect the average values across these models. Correction for multiple comparisons was performed through consideration of the familywise error rate ( $p < .05$ ).

Model	Size (mm <sup>3</sup> )	x	y	z	t	BA	Region
The Evidence-Independent (EI) Function							
430	38	22	−6	19.04	47		Insula_R
172	−12	12	−4	14.43	25		VentralStriatum
522	28	−64	44	14.08	7		Angular_R
72	−26	−68	38	13.51	7		Occipital_Mid_L
860	4	16	44	13.36	32		Cingulum_Mid_R
63	46	14	32	13.05	44		Frontal_Inf_Oper_R
187	−34	18	−2	12.32	47		Insula_L
279	−28	−52	46	11.43	7		Parietal_Inf_L
180	12	12	4	10.77	25		Caudate_R
42	−2	6	32	10.52	24		Cingulum_Mid_L
109	−4	−30	32	10.51	23		Cingulum_Mid_L
17	46	4	38	10.4	6		Precentral_R
44	2	−56	−36	10.39	−		Vermis_9
98	6	−64	48	10.16	7		Precuneus_R
31	10	28	28	9.76	32		Cingulum_Ant_R
19	−42	0	32	9.68	6		Precentral_L
50	−10	−72	44	9.51	7		Precuneus_L
42	−6	−80	−26	9.49	−		Cerebellum_Crus2_L
27	−40	−58	−36	9.45	−		Cerebellum_Crus1_L
27	8	−70	−28	9.09	−		Vermis_7
20	−32	−66	−30	9.05	19		Cerebellum_Crus1_L
36	50	−42	52	8.81	40		Parietal_Inf_R
23	48	28	28	8.73	45		Frontal_Inf_Tri_R

## References

- Basten, U., Biele, G., Heekeren, H.R., Fiebach, C.J., 2010. How the brain integrates costs and benefits during decision making. *Proc. Natl. Acad. Sci. U. S. A.* 107 (50), 21767–21772. <http://dx.doi.org/10.1073/pnas.0908104107>.
- Bogacz, R., Wagenmakers, E.J., Forstmann, B.U., Nieuwenhuis, S., 2010. The neural basis of the speed–accuracy tradeoff. *Trends Neurosci.* 33 (1), 10–16. <http://dx.doi.org/10.1016/j.tins.2009.09.002>.
- Bowman, N.E., Kording, K.P., Gottfried, J.A., 2012. Temporal integration of olfactory perceptual evidence in human orbitofrontal cortex. *Neuron* 75 (5), 916–927. <http://dx.doi.org/10.1016/j.neuron.2012.06.035>.
- Braunlich, K., Gomez-Lavin, J., Seger, C.A., 2015. Frontoparietal networks involved in categorization and item working memory. *NeuroImage* 107, 146–162. <http://dx.doi.org/10.1016/j.neuroimage.2014.11.051>.
- Buckner, R.L., 1998. Event-related fMRI and the hemodynamic response. *Hum. Brain Mapp.* 6 (5–6), 373–377.
- Buckner, R.L., Krienen, F.M., Yeo, B.T.T., 2013. Opportunities and limitations of intrinsic functional connectivity MRI. *Nat. Neurosci.* 16 (7), 832–837. <http://dx.doi.org/10.1038/nn.3423>.
- Cantwell, G., Crossley, M.J., Ashby, F.G., 2015. Multiple stages of learning in perceptual categorization: evidence and neurocomputational theory. *Psychon. Bull. Rev.* 1–16.
- Chance, F.S., Abbott, L.F., Reyes, A.D., 2002. Gain modulation from background synaptic input. *Neuron* 35, 773–782.
- Christophel, T.B., Hebart, M.N., Haynes, J.-D., 2012. Decoding the contents of visual short-term memory from human visual and parietal cortex. *J. Neurosci.* 32 (38), 12983–12989. <http://dx.doi.org/10.1523/JNEUROSCI.0184-12.2012>.
- Chumbley, J.R., Friston, K.J., 2009. False discovery rate revisited: FDR and topological inference using Gaussian random fields. *NeuroImage* 44 (1), 62–70. <http://dx.doi.org/10.1016/j.neuroimage.2008.05.021>.
- Churchland, A., Kiani, R., Shadlen, M., 2008. Decision-making with multiple alternatives. *Nat. Neurosci.* 11 (6), 693–702 (Retrieved from <http://www.nature.com/neuro/journal/v11/n6/abs/nn.2123.html>).
- Ciamelli, E., Grady, C.L., Moscovitch, M., 2008. Top-down and bottom-up attention to memory: a hypothesis (AtoM) on the role of the posterior parietal cortex in memory retrieval. *Neuropsychologia* 46 (7), 1828–1851. <http://dx.doi.org/10.1016/j.neuropsychologia.2008.03.022>.
- Cisek, P., Puskas, G.A., El-Murr, S., 2009. Decisions in changing conditions: the urgency-gating model. *J. Neurosci.* 29 (37), 11560–11571. <http://dx.doi.org/10.1523/JNEUROSCI.1844-09.2009>.
- Cohen, J.D., McClure, S.M., Yu, A.J., 2007. Should I stay or should I go? How the human brain manages the trade-off between exploitation and exploration. *Philos. Trans. R. Soc. Lond. Ser. B Biol. Sci.* 362 (1481), 933–942. <http://dx.doi.org/10.1098/rstb.2007.2098>.
- Daw, N.D., Gershman, S.J., Seymour, B., Dayan, P., Dolan, R.J., 2011. Model-based influences on humans' choices and striatal prediction errors. *Neuron* 69 (6), 1204–1215. <http://dx.doi.org/10.1016/j.neuron.2011.02.027>.
- De Martino, B., Fleming, S.M., Garrett, N., Dolan, R.J., 2013. Confidence in value-based choice. *Nat. Neurosci.* 16 (1), 105–110. <http://dx.doi.org/10.1038/nn.3279>.
- den Ouden, H.E.M., Daunizeau, J., Roiser, J., Friston, K.J., Stephan, K.E., 2010. Striatal prediction error modulates cortical coupling. *J. Neurosci.* 30 (9), 3210–3219. <http://dx.doi.org/10.1523/JNEUROSCI.4458-09.2010>.
- Ding, L., Gold, J.I., 2010. Caudate encodes multiple computations for perceptual decisions. *J. Neurosci.* 30 (47), 15747–15759. <http://dx.doi.org/10.1523/JNEUROSCI.2894-10.2010>.
- Ding, L., Gold, J.I., 2012. Neural correlates of perceptual decision making before, during, and after decision commitment in monkey frontal eye field. *Cereb. Cortex* 22 (5), 1052–1067. <http://dx.doi.org/10.1093/cercor/bhr178>.
- Ditterich, J., 2006a. Evidence for time-variant decision making. *Eur. J. Neurosci.* 24 (12), 3628–3641. <http://dx.doi.org/10.1111/j.1460-9568.2006.05221.x>.
- Ditterich, J., 2006b. Stochastic models of decisions about motion direction: behavior and physiology. *Neural Netw.* 19 (8), 981–1012. <http://dx.doi.org/10.1016/j.neunet.2006.05.042>.
- Douglas, R.J., Koch, C., Mahowald, M., Martin, K.A., Suarez, H.H., 1995. Recurrent excitation in neocortical circuits. *Science* 269 (5226), 981–985.
- Dunovan, K.E., Tremel, J.J., Wheeler, M.E., 2014. Prior probability and feature predictability interactively bias perceptual decisions. *Neuropsychologia* 61, 210–221. <http://dx.doi.org/10.1016/j.neuropsychologia.2014.06.024>.
- Fetsch, C.R., Kiani, R., Newsome, W.T., Shadlen, M.N., 2014. Effects of cortical microstimulation on confidence in a perceptual decision. *Neuron* 83 (4), 797–804. <http://dx.doi.org/10.1016/j.neuron.2014.07.011>.
- Fetsch, C.R., Kiani, R., Shadlen, M., 2015. Predicting the accuracy of a decision: a neural mechanism of confidence. *Cold Spring Harb. LXXIX*. <http://dx.doi.org/10.1101/sqb.2014.79.024893>.
- Fitzgerald, J.K., Freedman, D.J., Assad, J.A., 2011. Generalized associative representations in parietal cortex. *Nat. Neurosci.* 14 (8), 1075–1079. <http://dx.doi.org/10.1038/nn.2878>.
- Fleming, S.M., Maniscalco, B., Ko, Y., Amendi, N., Lau, H., 2015. Action-specific disruption of perceptual confidence. *Psychol. Sci.* 26 (1), 89–98.
- Freedman, D.J., Assad, J.A., 2006. Experience-dependent representation of visual categories in parietal cortex. *Nature* 443 (7107), 85–88. <http://dx.doi.org/10.1038/nature05078>.
- Friston, K.J., Mechelli, A., Turner, R., Price, C.J., 2000. Nonlinear responses in fMRI: the balloon model, Volterra kernels, and other hemodynamics. *NeuroImage* 12 (4), 466–477. <http://dx.doi.org/10.1006/nimg.2000.0630>.
- Gelman, A., Jakulin, A., Pittau, M.G., Su, Y.-S., 2008. A weakly informative default prior distribution for logistic and other regression models. *Ann. Appl. Stat.* 2 (4), 1360–1383. <http://dx.doi.org/10.1214/08-AOAS191>.
- Gherman, S., Philiastides, M.G., 2014. Neural representations of confidence emerge from the process of decision formation during perceptual choices. *NeuroImage* 106C, 134–143. <http://dx.doi.org/10.1016/j.neuroimage.2014.11.036>.
- Glimcher, P.W., Sparks, D.L., 1992. Movement selection in advance of action in the superior colliculus. *Nature* 355 (6360), 542–545. <http://dx.doi.org/10.1038/355542a0>.
- Gluck, M.A., Shohamy, D., Myers, C., 2002. How do people solve the “weather prediction” task? Individual variability in strategies for probabilistic category learning. *Learn. Mem.* 9 (6), 408–418. <http://dx.doi.org/10.1101/lm.45202>.
- Gluth, S., Rieskamp, J., Büchel, C., 2012. Deciding when to decide: time-variant sequential sampling models explain the emergence of value-based decisions in the human brain. *J. Neurosci.* 32 (31), 10686–10698. <http://dx.doi.org/10.1523/JNEUROSCI.0727-12.2012>.
- Gold, J.I., Shadlen, M.N., 2003. The influence of behavioral context on the representation of a perceptual decision in developing oculomotor commands. *J. Neurosci.* 23 (2), 632–651 Retrieved from <http://www.ncbi.nlm.nih.gov/pubmed/12533623>.
- Gold, J.I., Shadlen, M.N., 2007. The neural basis of decision making. *Annu. Rev. Neurosci.* 30, 535–574. <http://dx.doi.org/10.1146/annurev.neuro.29.051605.113038>.
- Grinband, J., Wager, T.D., Lindquist, M., Ferrera, V.P., Hirsch, J., 2008. Detection of time-varying signals in event-related fMRI designs. *NeuroImage* 43 (3), 509–520. <http://dx.doi.org/10.1016/j.neuroimage.2008.07.065>.
- Hanks, T.D., Mazurek, M.E., Kiani, R., Hopp, E., Shadlen, M.N., 2011. Elapsed decision time affects the weighting of prior probability in a perceptual decision task. *J. Neurosci.* 31 (17), 6339–6352. <http://dx.doi.org/10.1523/JNEUROSCI.5613-10.2011>.
- Hanks, T.D., Kiani, R., Shadlen, M.N., 2014. A neural mechanism of speed–accuracy tradeoff in macaque area LIP. *eLife* 2014, 1–17. <http://dx.doi.org/10.7554/eLife.02260>.
- Hebart, M.N., Schriever, Y., Donner, T.H., Haynes, J.-D., 2014. The relationship between perceptual decision variables and confidence in the human brain. *Cereb. Cortex* <http://dx.doi.org/10.1093/cercor/bhu181>.
- Heekeren, H.R., Marrett, S., Bandettini, P.A., Ungerleider, L.G., 2004. A general mechanism for perceptual decision-making in the human brain. *Nature* 431 (7010), 859–862. <http://dx.doi.org/10.1038/nature02966>.
- Heekeren, H.R., Marrett, S., Ruff, D.A., Bandettini, P.A., Ungerleider, L.G., 2006. Involvement of human left dorsolateral prefrontal cortex in perceptual decision making is independent of response modality. *Proc. Natl. Acad. Sci. U. S. A.* 103 (26), 10023–10028. <http://dx.doi.org/10.1073/pnas.0603949103>.
- Heitz, R.P., Schall, J.D., 2012. Neural mechanisms of speed–accuracy tradeoff. *Neuron* 76 (3), 616–628. <http://dx.doi.org/10.1016/j.neuron.2012.08.030>.
- Insabato, A., Pannunzi, M., Rolls, E.T., Deco, G., 2010. Confidence-related decision making. *J. Neurophysiol.* 104, 539–547. <http://dx.doi.org/10.1152/jn.01068.2009>.
- Jeung, S.K., 2014. Flexible Visual Information Representation in Human Parietal Cortex Harvard University.
- Kepecs, A., Mainen, Z.F., 2012. A computational framework for the study of confidence in humans and animals. *Philos. Trans. R. Soc. Lond. Ser. B Biol. Sci.* 367 (1594), 1322–1337. <http://dx.doi.org/10.1098/rstb.2012.0037>.
- Kepecs, A., Uchida, N., Zariwala, H.A., Mainen, Z.F., 2008. Neural correlates, computation and behavioural impact of decision confidence. *Nature* 455 (7210), 227–231. <http://dx.doi.org/10.1038/nature07200>.

- Kiani, R., Shadlen, M.N., 2009. Representation of confidence associated with a decision by neurons in the parietal cortex. *Science* 324, 759–764. <http://dx.doi.org/10.1126/science.1169405>.
- Kira, S., Yang, T., Shadlen, M.N., Kira, S., Yang, T., Shadlen, M.N., 2015. A neural implementation of Wald's sequential probability ratio test. *Neuron* 85, 1–13. <http://dx.doi.org/10.1016/j.neuron.2015.01.007>.
- Lak, A., Costa, G.M., Romberg, E., Koulakov, A.A., Mainen, Z.F., Kepecs, A., 2014. Orbitofrontal cortex is required for optimal waiting based on decision confidence. *Neuron* 84 (1), 190–201. <http://dx.doi.org/10.1016/j.neuron.2014.08.039>.
- Lo, C.-C., Wang, X.-J., 2006. Cortico-basal ganglia circuit mechanism for a decision threshold in reaction time tasks. *Nat. Neurosci.* 9 (7), 956–963. <http://dx.doi.org/10.1038/nn1722>.
- Logothetis, N.K., 2008. What we can do and what we cannot do with fMRI. *Nature* 453 (7197), 869–878. <http://dx.doi.org/10.1038/nature06976>.
- Lopez-Paniagua, D., Seger, C.A., 2011. Interactions within and between corticostriatal loops during component processes of category learning. *J. Cogn. Neurosci.* 23 (10), 3068–3083. [http://dx.doi.org/10.1162/jocn\\_a.00008](http://dx.doi.org/10.1162/jocn_a.00008).
- Marr, D., 1982. *Vision*. W. H. Freeman and Co, San Francisco.
- Medford, N., Critchley, H.D., 2010. Conjoint activity of anterior insular and anterior cingulate cortex: awareness and response. *Brain Struct. Funct.* 214 (5–6), 535–549. <http://dx.doi.org/10.1007/s00429-010-0265-x>.
- Meeter, M., Myers, C.E., Shohamy, D., Hopkins, R.O., Gluck, M.A., 2006. Strategies in probabilistic categorization: results from a new way of analyzing performance. *Learn. Mem.* 13, 230–239. <http://dx.doi.org/10.1101/lm.43006.1>.
- Menon, V., 2011. Large-scale brain networks and psychopathology: a unifying triple network model. *Trends Cogn. Sci.* 15 (10), 483–506. <http://dx.doi.org/10.1016/j.tics.2011.08.003>.
- Menon, V., Uddin, L., 2010. Saliency, switching, attention and control: a network model of insula function. *Brain Struct. Funct.* 214, 655–667. <http://dx.doi.org/10.1007/s00429-010-0262-0>. Saliency.
- Mumford, J., Poline, J.-B., Poldrack, R., 2015. Orthogonalization of regressors in fMRI models. *PLoS ONE* 10 (4), e0126255. <http://dx.doi.org/10.1371/journal.pone.0126255>.
- Niyogi, R.K., Wong-Lin, K., 2013. Dynamic excitatory and inhibitory gain modulation can produce flexible, robust and optimal decision-making. *PLoS Comput. Biol.* 9 (6), e1003099. <http://dx.doi.org/10.1371/journal.pcbi.1003099>.
- Nosofsky, R.M., 1986. Attention, similarity, and the identification-categorization relationship. *J. Exp. Psychol. Gen.* 115 (1), 39–61 (Retrieved from <http://www.ncbi.nlm.nih.gov/pubmed/2937873>).
- Nosofsky, R.M., Little, D.R., James, T.W., 2012. Activation in the neural network responsible for categorization and recognition reflects parameter changes. *Proc. Natl. Acad. Sci.* 109 (1), 333–338. <http://dx.doi.org/10.1073/pnas.1111304109>.
- Padoa-Schioppa, C., 2011. Neurobiology of economic choice: a good-based model. *Annu. Rev. Neurosci.* 34, 333–359. <http://dx.doi.org/10.1146/annurev-neuro-061010-113648>. NEUROBIOLOGY.
- Palmer, J., Huk, A.C., Shadlen, M.N., 2005. The effect of stimulus strength on the speed and accuracy of a perceptual decision. *J. Vis.* 5 (5), 376–404. <http://dx.doi.org/10.1167/5.5.1>.
- Pastor-Bernier, A., Cisek, P., 2011. Neural correlates of biased competition in premotor cortex. *J. Neurosci.* 31 (19), 7083–7088. <http://dx.doi.org/10.1523/JNEUROSCI.5681-10.2011>.
- Penny, W.D., 2012. Comparing dynamic causal models using AIC, BIC and free energy. *NeuroImage* 59 (1), 319–330. <http://dx.doi.org/10.1016/j.neuroimage.2011.07.039>.
- Philastides, M.G., Biele, G., Heekeren, H., 2010. A mechanistic account of value computation in the human brain. *Proc. Natl. Acad. Sci.* 107 (20), 9430–9435. <http://dx.doi.org/10.1073/pnas.1001732107>. DCSupplemental. [www.pnas.org/cgi/doi/10.1073/pnas.1001732107](http://www.pnas.org/cgi/doi/10.1073/pnas.1001732107).
- Philastides, M.G., Auksztulewicz, R., Heekeren, H.R., Blankenburg, F., 2011. Causal role of dorsolateral prefrontal cortex in human perceptual decision making. *Curr. Biol.* 21 (11), 980–983. <http://dx.doi.org/10.1016/j.cub.2011.04.034>.
- Pleskac, T.J., Busemeyer, J.R., 2010. Two-stage dynamic signal detection: a theory of choice, decision time, and confidence. *Psychol. Rev.* 117 (3), 864–901. <http://dx.doi.org/10.1037/a0022399>.
- Ploran, E.J., Nelson, S.M., Velanova, K., Donaldson, D.I., Petersen, S.E., Wheeler, M.E., 2007. Evidence accumulation and the moment of recognition: dissociating perceptual recognition processes using fMRI. *J. Neurosci.* 27 (44), 11912–11924. <http://dx.doi.org/10.1523/JNEUROSCI.3522-07.2007>.
- Ploran, E.J., Tremel, J.J., Nelson, S.M., Wheeler, M.E., 2011. High quality but limited quantity perceptual evidence produces neural accumulation in frontal and parietal cortex. *Cereb. Cortex* 21 (11), 2650–2662. <http://dx.doi.org/10.1093/cercor/bhr055>.
- Poldrack, R.A., Prabhakaran, V., Seger, C.A., Gabrieli, J.D., 1999. Striatal activation during acquisition of a cognitive skill. *Neuropsychology* 13 (4), 564–574 (Retrieved from <http://www.ncbi.nlm.nih.gov/pubmed/10527065>).
- Ratcliff, R., 1978. A theory of memory retrieval. *Psychol. Rev.* 85 (2), 59–108 (Retrieved from <http://psycnet.apa.org/journals/rev/85/2/59/>).
- Reddi, B.A., Carpenter, R.H., 2000. The influence of urgency on decision time. *Nat. Neurosci.* 3 (8), 827–830. <http://dx.doi.org/10.1038/77739>.
- Rigoux, L., Stephan, K.E., Friston, K.J., Daunizeau, J., 2014. Bayesian model selection for group studies—revisited. *NeuroImage* 84, 971–985. <http://dx.doi.org/10.1016/j.neuroimage.2013.08.065>.
- Rolls, E.T., Grabenhorst, F., Deco, G., 2010a. Choice, difficulty, and confidence in the brain. *NeuroImage* 53 (2), 694–706. <http://dx.doi.org/10.1016/j.neuroimage.2010.06.073>.
- Rolls, E.T., Grabenhorst, F., Deco, G., 2010b. Decision-making, errors, and confidence in the brain. *J. Neurophysiol.* 104 (5), 2359–2374. <http://dx.doi.org/10.1152/jn.00571.2010>.
- Rosa, M.J., Bestmann, S., Harrison, L., Penny, W., 2010. Bayesian model selection maps for group studies. *NeuroImage* 49 (1), 217–224. <http://dx.doi.org/10.1016/j.neuroimage.2009.08.051>.
- Salinas, E., Abbott, L.F., 1996. A model of multiplicative neural responses in parietal cortex. *Proc. Natl. Acad. Sci. U. S. A.* 93 (21), 11956–11961 (Retrieved from <http://www.pubmedcentral.nih.gov/articlerender.fcgi?artid=38165&tool=pmcentrez&rendertype=abstract>).
- Salinas, E., Thier, P., 2000. Gain modulation: a major computational principle of the central nervous system. *Neuron* 27, 15–21.
- Schwartenbeck, P., FitzGerald, T.H.B., Mathys, C., Dolan, R., Friston, K., 2014. The dopaminergic midbrain encodes the expected certainty about desired outcomes. *Cereb. Cortex* 1–12. <http://dx.doi.org/10.1093/cercor/bhu159>.
- Seger, C.A., Peterson, E.J., Cincotta, C.M., Lopez-Paniagua, D., Anderson, C.W., 2010. Dissociating the contributions of independent corticostriatal systems to visual categorization learning through the use of reinforcement learning modeling and Granger causality modeling. *NeuroImage* 50 (2), 644–656. <http://dx.doi.org/10.1016/j.neuroimage.2009.11.083>.
- Seger, C.A., Braunlich, K., Wehe, H., Liu, Z., 2015. Generalization in category learning: the roles of representational and decisional uncertainty. *J. Neurosci.* 35 (23), 8802–8812.
- Sereno, M.I., Pitzalis, S., Martinez, A., 2001. A mapping of contralateral space in retinotopic coordinates by a parietal cortical area in humans. *Science* 294, 1350–1354.
- Shadlen, M.N., Newsome, W., 2001. Neural basis of a perceptual decision in the parietal cortex (area LIP) of the rhesus monkey. *J. Neurophysiol.* 1916–1936 (Retrieved from <http://jn.physiology.org/content/86/4/1916.short>).
- Shadlen, M.N., Kiani, R., Hanks, T.D., Churchland, A.K., 2008. Neurobiology of decision making: an intentional framework. In: Engel, C., Singer, W. (Eds.), *Better than Conscious? Decisions Making, the Human Mind, and Implications for Institutions*. MIT Press, Cambridge, pp. 71–101.
- Shohamy, D., Myers, C.E., Kalanithi, J., Gluck, M., 2008. Basal ganglia and dopamine contributions to probabilistic category learning. *Neurosci. Biobehav. Rev.* 32 (2), 219–236. <http://dx.doi.org/10.1016/j.neubiorev.2007.07.008>. Basal.
- Sigala, N., Logothetis, N.K., 2002. Visual categorization shapes feature selectivity in the primate temporal cortex. *Nature* 415 (6869), 318–320. <http://dx.doi.org/10.1038/415318a>.
- Simen, P., 2012. Evidence accumulator or decision threshold—which cortical mechanism are we observing? *Front. Psychol.* 3 (June), 183. <http://dx.doi.org/10.3389/fpsyg.2012.00183>.
- Smith, P.L., Ratcliff, R., 2004. Psychology and neurobiology of simple decisions. *Trends Neurosci.* 27 (3), 161–168. <http://dx.doi.org/10.1016/j.tins.2004.01.006>.
- Smith, D.V., Hayden, B.Y., Truong, T.-K., Song, A.W., Platt, M.L., Huettel, S.A., 2010. Distinct value signals in anterior and posterior ventromedial prefrontal cortex. *J. Neurosci.* 30 (7), 2490–2495. <http://dx.doi.org/10.1523/JNEUROSCI.3319-09.2010>.
- Spiering, B., Ashby, F., 2008. Response processes in information-integration category learning. *Neurobiol. Learn. Mem.* 90 (2), 330–338. <http://dx.doi.org/10.1016/j.nlm.2008.04.015>. Response.
- Sridharan, D., Levitin, D.J., Menon, V., 2008. A critical role for the right fronto-insular cortex in switching between central-executive and default-mode networks. *Proc. Natl. Acad. Sci. U. S. A.* 105 (34), 12569–12574. <http://dx.doi.org/10.1073/pnas.0800005105>.
- Standage, D., You, H., Wang, D.-H., Dorris, M.C., 2011. Gain modulation by an urgency signal controls the speed–accuracy trade-off in a network model of a cortical decision circuit. *Front. Comput. Neurosci.* 5, 7. <http://dx.doi.org/10.3389/fncom.2011.00007>.
- Standage, D., You, H., Wang, D.-H., Dorris, M.C., 2013. Trading speed and accuracy by coding time: a coupled-circuit cortical model. *PLoS Comput. Biol.* 9 (4), e1003021. <http://dx.doi.org/10.1371/journal.pcbi.1003021>.
- Standage, D., Blohm, G., Dorris, M.C., 2014a. On the neural implementation of the speed–accuracy trade-off. *Front. Neurosci.* 8, 236. <http://dx.doi.org/10.3389/fnins.2014.00236>.
- Standage, D., Wang, D.-H., Blohm, G., 2014b. Neural dynamics implement a flexible decision bound with a fixed firing rate for choice: a model-based hypothesis. *Front. Neurosci.* 8, 318. <http://dx.doi.org/10.3389/fnins.2014.00318>.
- Stephan, K., Penny, W., Daunizeau, J., 2009. Bayesian model selection for group studies. *NeuroImage* 46 (4), 1004–1017. <http://dx.doi.org/10.1016/j.neuroimage.2009.03.025>. Bayesian.
- Sutton, R.S., Barto, A.G., 1998. *Reinforcement Learning: An Introduction*.
- Swaminathan, S.K., Freedman, D.J., 2012. Preferential encoding of visual categories in parietal cortex compared with prefrontal cortex. *Nat. Neurosci.* 15 (2), 315–320. <http://dx.doi.org/10.1038/nn.3016>.
- Thura, D., Cisek, P., 2014. Deliberation and commitment in the premotor and primary motor cortex during dynamic decision making. *Neuron* 81 (6), 1401–1416. <http://dx.doi.org/10.1016/j.neuron.2014.01.031>.
- Thura, D., Beauregard-Racine, J., Fradet, C.-W., Cisek, P., 2012. Decision-making by urgency-gating: theory and experimental support. *J. Neurophysiol.* 108, 2912–2930. <http://dx.doi.org/10.1152/jn.01071.2011>.
- Tobler, P.N., O'Doherty, J.P., Dolan, R.J., Schultz, W., 2007. Reward value coding distinct from risk attitude-related uncertainty coding in human reward systems. *J. Neurophysiol.* 97 (2), 1621–1632. <http://dx.doi.org/10.1152/jn.00745.2006>.
- Tremel, J.J., Wheeler, M.E., 2015. Content-specific evidence accumulation in inferior temporal cortex during perceptual decision-making. *NeuroImage* <http://dx.doi.org/10.1016/j.neuroimage.2014.12.072>.
- Vickers, D., Packer, J., 1982. Effects of alternating set for speed or accuracy on response time, accuracy and confidence in a unidimensional discrimination task. *Acta Psychol.* 50, 179–197. [http://dx.doi.org/10.1016/0001-6918\(82\)90006-3](http://dx.doi.org/10.1016/0001-6918(82)90006-3).
- Waldschmidt, J.G., Ashby, F.G., 2011. Cortical and striatal contributions to automaticity in information-integration categorization. *NeuroImage* 56 (3), 1791–1802. <http://dx.doi.org/10.1016/j.neuroimage.2011.02.011>.
- Wheeler, M., Woo, S., Ansel, T., Tremel, J., Collier, A.L., Velanova, K., ... Yang, T., 2014. The strength of gradually accruing probabilistic evidence modulates brain activity during a categorical decision. *J. Cogn. Neurosci.* 27 (4), 705–719. <http://dx.doi.org/10.1162/jocn.2013.01801>.
- Yang, T., Shadlen, M.N., 2007. Probabilistic reasoning by neurons. *Nature* 447 (7148), 1075–1080. <http://dx.doi.org/10.1038/nature05852>.